2008

Photofragmentation of SiF4 upon Si 2p and F 1s Core Excitation: Cation and Anion Yield Spectroscopy

Maria Novella Piancastelli
Uppsala University, maria-novella.piancastelli@physics.uu.se

Wayne C. Stolte
University of Nevada, Las Vegas, wcstolte@lbl.gov

Renaud Guillemin
CNRS, Laboratoire de Chimie Physique-Matière et Rayonnement

A. Wolska
Institute of Physics, Polish Academy of Sciences

Dennis W. Lindle
University of Nevada, Las Vegas, lindle@unlv.nevada.edu

Photofragmentation of SiF4 upon Si 2p and F 1s core excitation: Cation and anion yield spectroscopy

M. N. Piancastelli, W. C. Stolte, R. Guillemin, A. Wolska, and D. W. Lindle

Citation: J. Chem. Phys. **128**, 134309 (2008); doi: 10.1063/1.2851135
View online: http://dx.doi.org/10.1063/1.2851135
View Table of Contents: http://jcp.aip.org/resource/1/JCPSA6/v128/i13
Published by the American Institute of Physics.

Photofragmentation of SiF_4 upon Si 2*p* and F 1*s* core excitation: Cation and anion yield spectroscopy

M. N. Piancastelli,[1,a)] W. C. Stolte,[2] R. Guillemin,[3] A. Wolska,[4] and D. W. Lindle[2]
[1]*Physics Department, Uppsala University, 751 21 Uppsala, Sweden*
[2]*Department of Chemistry, University of Nevada, Las Vegas, Nevada 89154-4003, USA*
[3]*Laboratoire de Chimie-Physique-Matière et Rayonnement, Université Pierre et Marie Curie, 75231 Paris Cedex 05, France*
[4]*Institute of Physics, PAS, A1. Lotnikow 32/46, 02-668 Warsaw, Poland*

(Received 3 December 2007; accepted 23 January 2008; published online 4 April 2008)

We have studied the fragmentation dynamics of core-excited SiF_4 by means of soft-x-ray photoexcitation and partial positive and negative ion yield measurements around the Si $L_{2,3}$-shell and F *K*-shell ionization thresholds. All detectable ionic fragments are reported and we observe significant differences between the various partial ion yields near the Si 2*p* threshold. The differences are similar to our previous results from CH_3Cl showing more extended fragmentation in correspondence to transitions to Rydberg states. At variance with smaller systems, we observe negative ion production in the shape resonance region. This can be related to the possibility in a relatively large system to dissipate positive charge over several channels. © *2008 American Institute of Physics*. [DOI: 10.1063/1.2851135]

INTRODUCTION

Silicon tetrafluoride belongs to the group of highly symmetric, stable systems, with a central atom surrounded by strongly electronegative ligands, which have attracted considerable attention in the literature because those are showcases describing the existence and properties of the continuum resonances known as shape resonances.[1] Namely, the absorption spectra of SiF_4 around both the Si 2*p* and the F 1*s* ionization thresholds show intense molecular resonances above and below both thresholds. Such phenomena are connected to the existence of an effective potential barrier which forms an inner well and an outer well. The quasibound continuum states known as shape resonances are located in the inner well. A shape resonance can be described as a continuum state supported by the potential barrier in which the emitted photoelectron is temporarily trapped, eventually tunneling through and ejected into the continuum.[2] An alternative but equivalent description is electron excitation to virtual molecular orbitals pushed above the ionization threshold by the potential barrier.[3] Both models give essentially the same picture.

The scattering picture can be more useful when describing changes in electron angular momentum in the region of a shape resonance, while the molecular orbital picture can be more appropriate to describe the continuum resonances in terms of symmetry and selection rules. In fact, continuum resonances were first observed in the spectra of Si and S *L* edge of SiF_4 (Ref. 4) and SF_6 (Ref. 5) and interpreted as due to a barrier in the molecular potential created by the fluorine cage surrounding the central atom. In this widespread and, at some extent, simplified picture, the barrier then subdivides the effective scattering potential into inner-well and outer-well regions, the former supporting quasibound orbitals in the continuum,[1] giving rise to scattering resonances traditionally known as shape resonances.

The ever high interest in the spectroscopic properties of SiF_4 are also justified by its technological importance as it is routinely employed as an etchant in microelectronics, representing thus one of the more relevant technological silicon compounds.[6]

Experimental work on SiF_4 performed over almost three decades has nearly covered its whole electronic spectrum by employing a variety of techniques, including absorption, fluorescence, photoionization, and scattering experiments.

Photoabsorption data in the near threshold range were provided by Suto *et al.*[7] and Kameta *et al.*[8] Valence photoionization has been the subject of recent works by Cooper *et al.*[9] and Holland *et al.*,[10] who reported photoelectron angular distributions, partial photoionization cross sections, and branching ratios for the first five valence ionizations as an extension of a previous work by Yates *et al.*[11]

Absolute photoabsorption oscillator strengths for valence excitation loss spectroscopy in the dipole regime have also been provided.[12–14]

Photoionization and electron-impact studies below threshold and in the Si 2*p* ionization continua performed by several investigators[15–21] provided an interpretation for the resonant and normal Auger spectra[22] and helped in clarifying the relative importance of several decay channels for discrete Si 2*p* and 2*s* excitations and for the shape resonant states in the Si 2*p* continua. Several photoabsorption and photoionization studies were also performed in the vicinity of the Si 1*s* (Refs. 23 and 24) and F 1*s* ionizations.[15,25–28]

This relatively large abundance of experimental work has stimulated several theoretical investigations, either in the

a)Author to whom correspondence should be addressed. Electronic mail: maria-novella.piancastelli@fysik.uu.se.

molecular continuum with the use of the multiple-scattering formalism.[11,18,29–31] or for an interpretation of the photoelectron spectrum with *ab initio* methods such as third-order algebraic-diagrammatic construction, outer valence Green function, and configuration-interaction methods.[10,13] Even if the multiple-scattering calculations succeeded in interpreting most of the prominent features found in both valence[11,30] and core[18,29,30] photoabsorption and photoionization studies, the agreement with the various sets of experimental data is often only qualitative, especially in the near threshold region.[10,11,18,28] A recent comprehensive paper includes photoabsorption and photoionization cross section calculations for all valence and core levels with the time-dependent density-functional theory approach.[32]

Resonant excitation or ionization of a core electron by a photon in the soft-x-ray regime promotes a molecule to a rather unstable potential energy surface. The excited system relaxes on a very short time scale, typically tens of femtoseconds or less, most likely by emitting an electron, then adopting a different geometry and/or breaking one or several chemical bonds. Below the core-level ionization limits, electronic relaxation processes generally lead to singly charged ions, produced either by participator or spectator resonant Auger decay. Above the core-level ionization limits, the intermediate state is itself singly charged and relaxes preferentially by normal Auger decay, leading to doubly charged species. In rarer situations, emission of several electrons during the (resonant or not) Auger decay is possible. In each case, ion fragmentation is dependent on internal energy, i.e., upon the electronic and vibrational energies stored in the system: The more energy stored, the more the ion is likely to dissociate. These phenomena can be highlighted by detection of one or several emitted particles. High-resolution electron spectroscopy is a suitable tool in studying the ultrafast processes of electronic and nuclear rearrangements, whereas ion spectroscopy typically monitors processes taking place on longer time scales. However, one can obtain a wealth of information on the dynamics of core-excited species by analyzing partial ion yield spectra.

In the present work, we report experiments on partial ion yields upon core excitation around both the Si $2p$ and the F $1s$ core levels. All produced ions are collected, including minority species such as doubly and triply charged cations and anions. We demonstrated that in such a relatively large system, the production of anions is possible in the shape resonance region, in analogy with our previous results on another rather large molecule with electronegative ligands, SF_6,[33] and at variance with many smaller molecules [CO,[34] N_2O,[35] CO_2,[36] NO (Ref. 37)] where we showed that anion spectroscopy is a good tool for assigning shape resonances since in small systems, the production of anions following the fragmentation of doubly positively charged species is definitely unlikely, and therefore no spectral structures are evident in the anion yield curves at the shape resonance position. We also noticed that the shape resonances are clearly visible in the ion yields when the species is core excited around the Si $2p$ core level, while those are almost invisible when the excitation takes place around the F $1s$ core level, at variance with our previous results on SF_6. We attribute this finding to a more localized character of the continuum resonances around the central atom. We confirm our previous observation reported for other systems that the spectral region pertaining to the excitation to Rydberg states is more intense as a function of the extent of fragmentation.

EXPERIMENTAL

Our measurements were performed on the undulator beamline BL 8.0.1.3 at the Advanced Light Source, Lawrence Berkeley National Laboratory. The monochromator resolution on BL 8.0.1.3 around 100 eV was approximately 12–15 meV when using an entrance slit width of 12 μm and an exit slit width of 20 μm. We used an entrance slit width of 20 μm and an exit slit width of 30 μm near 700 eV, resulting in a lifetime-limited resolution. The experimental apparatus used in the present study has been previously described.[38] Basically, the apparatus consists of a 180° magnetic mass spectrometer, providing a full width at half maximum corresponding to a fraction of uma, which is adequate to distinguish fragments with sequential number of hydrogen atoms, a lens system to focus the ions created in the interaction region onto the entrance slit of the mass spectrometer, and a gas cell containing an extraction field to move the ions created in the interaction region into the lens system. The target gas enters the open cell via an effusive jet of 2 mm diameter. A channel electron multiplier is used at the exit slit of the spectrometer to detect the ions. Finally, a differential pumping system was used to isolate the target chamber vacuum (2×10^{-5} torr) from the beamline vacuum (1×10^{-9} torr). The SiF_4 gas was commercially obtained from Scott Specialty Gases, VLS1 grade, 99.998% purity, and used without further purification. Photon energies were calibrated at the Si $L_{2,3}$ edges using the Si $2p_{3/2}\rightarrow 6a_1^*$ resonance at 106.095 eV (Ref. 19) and verified with krypton between 90 and 94 eV,[20] and at the F K edge by the F $1s\rightarrow 6a_1^*$ resonance at 689.2 eV.[15] In order to obtain reasonable statistics and verify reproducibility, all of the spectra presented in this paper are the sum of several recordings, which were separately normalized, especially the weaker dissociation channels as the doubly charge ions and the anions for which up to ten spectra have been recorded and summed.

RESULTS AND DISCUSSION

When a core hole is induced in a molecule, dissociation is very likely to occur following or even during electronic relaxation. The main pathway to molecular fragmentation is the decay of the species with a core hole to a molecular ion with a single positive charge (mainly below threshold) or to a molecular ion with a double positive charge (mainly above threshold), which are often metastable and subsequently dissociate by breaking one or more chemical bonds. Observation of the resulting ions (molecular or atomic) is very informative of the nature of the excited or ionized state and of the dynamics of the photofragmentation process.

Silicon tetrafluoride has four equivalent Si–F bond in a tetrahedral geometry. The ground state configuration in the T_d symmetry point group is

$$\underbrace{(1a_1)^2}_{\text{Si } 1s}\underbrace{(1t_2)^6(2a_1)^2}_{\text{F } 1s}\underbrace{(3a_1)^2}_{\text{Si } 2s}\underbrace{(2t_2)^6}_{\text{Si } 2p}\underbrace{(4a_1)^2(3t_2)^6}_{\text{inner valence}}\underbrace{(5a_1)^2(4t_2)^6(1e)^4(5t_2)^6(1t_1)^6}_{\text{outer valence}}\underbrace{(6a_1^*)(6t_2^*)}_{\text{virtual valence}}.$$

The outer valence orbitals $5a_1$ and $4t_2$ are σ-bonding orbitals formed by superposition of Si $3s/3p$ and F $2s/2p$ orbitals, while the three outermost orbitals $1e$, $5t_2$, and $1t_1$ are halogen lone-pair p orbitals with small contributions from the Si $3d$ orbitals in the $1e$ and $5t_2$. The virtual valence orbitals are the corresponding σ^* (Si–F) levels.

We have performed ion yield measurements in the photon energy regions including the Si $2p$ and the F $1s$ ionization thresholds. All detectable fragments have been collected, both anions and cations.

Si 2*p* edge

In the photon energy region including the Si $L_{2,3}$ edges, we have detected the following charged fragments: SiF_3^+, SiF_2^+, SiF^+, Si^+, F_2^+, F^+, SiF_3^{++}, SiF_2^{++}, SiF^{++}, Si^{++}, F^{++}, Si^{+++}, Si^-, and F^-, and a total ion yield (TIY). We begin by analyzing the behavior of the singly positively charged species. We have also recorded the TIY for the sake of comparison. The parent ion was too heavy to be detected under our experimental conditions.

The absorption spectrum of SiF_4 around the Si $L_{2,3}$ edges has been reported by several authors.[16–21] We follow the assignment proposed by the high-resolution work of Ref. 20. In the photon energy region from 105 to 109 eV, broad features are observed, which are attributed to excitations into unoccupied valence orbitals. The two lowest-lying resonances at 106.095 and 106.650 eV are spin-orbit split $2p_{3/2}{}^{-1}6a_1{}^*$ and $2p_{1/2}{}^{-1}6a_1{}^*$ resonances. A diversity of assignments is given in the literature for the two following features at 108.360 and 108.800 eV;[19] most of them attribute these two peaks to excitations of t_2 symmetry.

At $h\nu > 109$ eV, excitations into much narrower states with a fine structure splitting are observed, which are assigned to vibrationally split Rydberg states. The lowest Rydberg states in the energy region from 109.1 to 110.2 eV are mainly attributed to $4s$ ($2p_{3/2}{}^{-1}4s$) and $4s'$ ($2p_{1/2}{}^{-1}4s$) core-excited states. These $4s$ and $4s'$ resonances look different from the excitation to higher Rydberg states, which can be attributed to a partial σ^* character stemming from Rydberg-valence mixing (see below). The spectral features observed for energies above 110.2 eV are mostly due to excitations into nd and nd' states, which can be described by approximately constant quantum defects as well as by similar intensity variation of the vibrational substates (see below). In addition, weak $4p$ and $4p'$ excitations are identified. The ionization thresholds for the two spin-orbit split states $2p_{3/2}{}^{-1}$ and $2p_{1/2}{}^{-1}$ fall at 111.740 and 112.350 eV. Above threshold, there are two features at 117 and 134.5 eV photon energies assigned as shape resonances of e and t_2 symmetries, respectively.[32]

In Figs. 1 and 2, we show the partial ion yields for the singly and multiply positive charged fragments. On the top, the TIY curve (equivalent to photoabsorption) is reported for the sake of comparison.

If we compare the singly charged fragments (Fig. 1) in

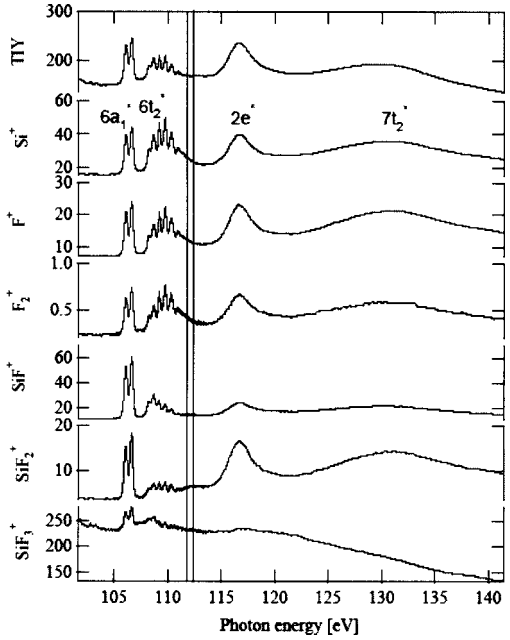

FIG. 1. Partial ion yields for all the singly positive charged fragments detected around the Si $2p$ edge. On the bottom, the TIY curve (equivalent to photoabsorption) is reported for the sake of comparison.

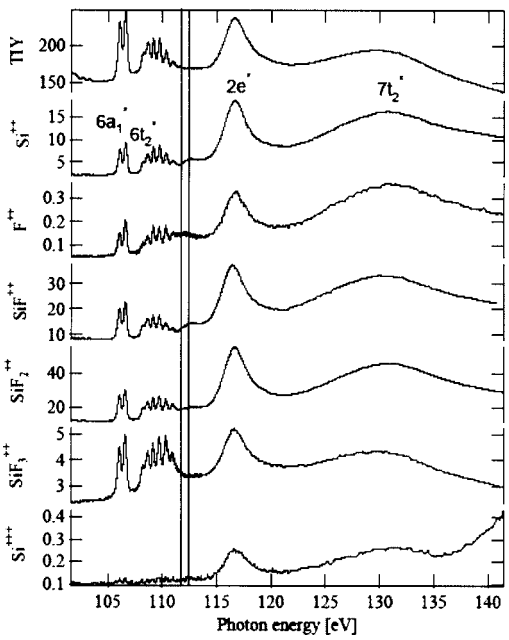

FIG. 2. Partial ion yields for all the multiply positive charged fragments detected around the Si $2p$ edge. On the bottom, the TIY curve is reported for the sake of comparison.

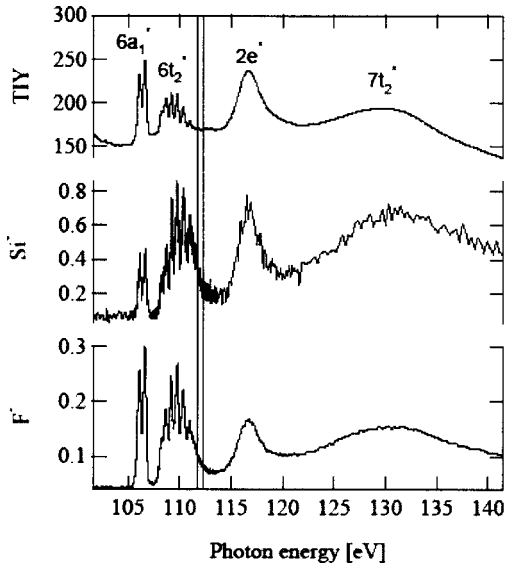

FIG. 3. Partial ion yields for all the negatively charged fragments detected around the Si 2*p* edge. On the bottom, the TIY curve is reported for the sake of comparison.

the photon energy region below threshold, we can observe that the Rydberg series is more prominent for the lighter fragments such as Si^+, F^+, and F_2^+, although we do not observe a definite trend in the relative increase in intensity of the spectral features related to Rydberg decay as a function of the fragment mass the same way we did in several other cases.[39–41] Above threshold, we see the features at 117 and 134.5 eV, assigned as shape resonances, in all curves, although again with more relative intensity for the lighter fragments. This observation is corroborated by the appearance of the yield curves of the multiply charged fragments, where the two peaks related to the shape resonances are much more evident due to the fact that the shape resonance decay produces doubly charged species as the first step, and therefore in such spectral region, we expect either doubly or multiply charges species or light fragments such as Si^+ and F^+ which can be produced simultaneously with other positively charged species following as a further step the Auger decay to a doubly charged species. This effect is well known and can be explained by the dominant decay pattern above threshold being normal Auger decay producing doubly charged cations. It is especially visible for spectral structures related to shape resonances because the intensity of the Auger decay mimics the resonant increase in relative intensity of the photoelectron lines, and therefore the resonant enhancement is visible in fragment-ion yields, such as doubly charged ions, reached after Auger emission.

In Fig. 3, we report the yield curves for the two anions we detect in the photon energy region, F^- and Si^-. The most interesting observation is that we see a rather significant production of anions in correspondence to the above threshold continuum resonances. The yield of the anion fragments detected in this photon energy region is particularly interesting. The most noticeable feature is that the shape resonances have spectral intensities in the anion yields comparable to those of the cation yields. This is in contrast to a series of previous investigations[34–37] where we discussed the possibility of using anion yields to assign above threshold resonances directly via experiment. This argument was based on the fact that to produce an anion following the normal Auger decay of a core hole, which leads initially to a doubly charged parent ion, a net concentration of triple positive charge on one fragment must be envisaged in a small molecule. In simple systems such as CO,[34] N_2O,[35] CO_2,[36] and NO,[37] this was found to be highly unlikely. We have also used this effect to build a purely experimental method to assign shape resonances versus other kinds of continuum resonances such as doubly excited states. However, while this argument is strong for diatomic or triatomic molecules, it does not necessarily hold for more complex systems, where the possibility for delocalization of positive charge exists. This quenching effect can therefore be directly related to the size of the investigated molecule: If the system is large enough, it is possible to observe anion yields at shape resonance positions. As an example, formation of F^- could stem from one of the following patterns, as well as many more not depicted here:

$$SiF_4^{2+} \rightarrow F^- + SiF_3^{3+}$$

$$F^- + SiF_3^{3+} + F^0$$

$$F^- + SiF_2^{2+} + F^+$$

$$F^- + SiF_2^{+} + F^{2+}.$$

We detect all the above mentioned species, except SiF_3^{3+}; therefore these pathways are reasonable.

We have already reported a similar finding for SF_6,[33] and the analogous observation in SiF_4 confirms the overall interpretation.

F 1*s* edge

The charged fragments we detect in the photon energy region near the F *K* edge are SiF_3^+, SiF_2^+, SiF^+, Si^+, F_2^+, F^+, SiF_3^{++}, SiF_2^{++}, SiF^{++}, Si^{++}, F^{++}, Si^{+++}, Si^-, and F^-. We did not gather a TIY spectrum for this energy range.

As a general observation, we notice that while at the Si 2*p* edge the overall appearance of the partial ion yields is rather similar, around the F 1*s* edge, there are much larger differences between the various yield curves. We attribute this general trend to the fact that in the former case, electron decay following core excitation reaches final states where the contribution of the central Si atom is large, and therefore are more symmetrically distributed over the molecule, while in the latter case, the final states are more localized on the peripheral F atoms. As a consequence, the subsequent fragmentation is more anisotropic at the F 1*s* edge.

In Fig. 4, we report the yield curves for all the singly positive charged fragments. The literature spectral assignment from angle-resolved ion yield measurements is as follows:[27] Vinogradov and Zimkina first observed the x-ray absorption spectra of the SiF_4 molecule.[4] They pointed out that the relative spacings of the absorption bands are almost identical between the spectra of the F 1*s* and Si 2*p* regions. Thus there are three intense features below the threshold,

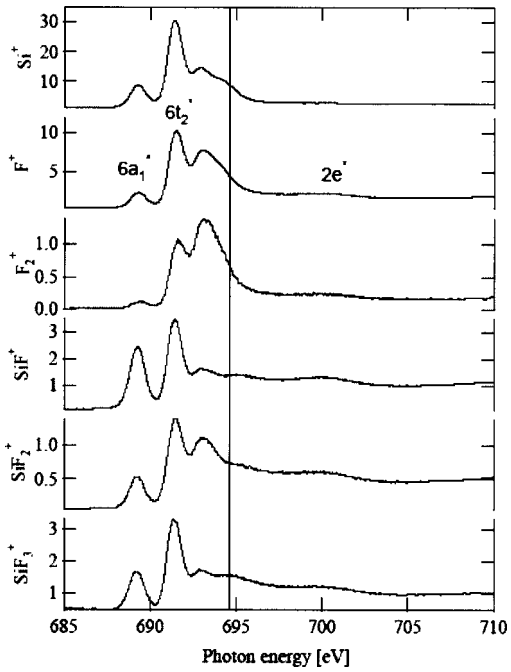

FIG. 4. Partial ion yields for all the singly positive charged fragments detected around the F 1*s* edge.

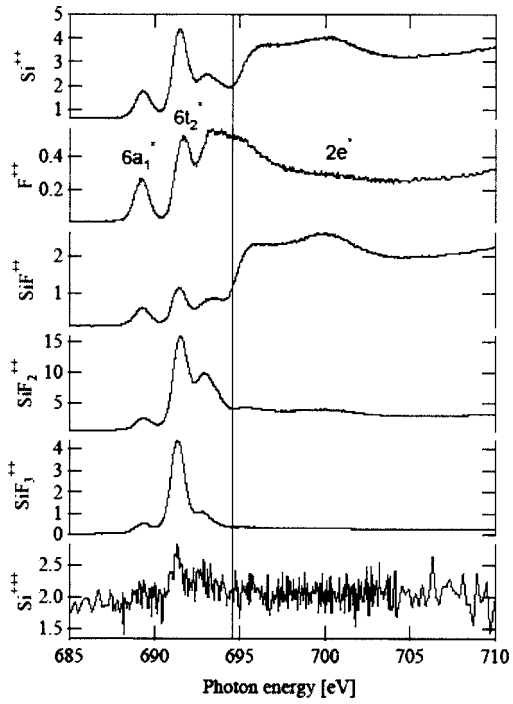

FIG. 5. Partial ion yields for all the multiply positive charged fragments detected around the F 1*s* edge.

whereas a broad feature is visible above the threshold. In analogy with the assignment for the structures below the Si 2*p* thresholds, we can assign the three below threshold features to F $1s \rightarrow 6a_1^*$, F $1s \rightarrow 6t_2^*$, and a composition of the overlapping transitions from F 1*s* to the Rydberg orbitals of various symmetries. On the ground of symmetry-resolved ion yield spectra,[28] it can be deduced that the second lowest-lying feature has a mixed valence-Rydberg character. The ionization threshold is at 694.56 eV. Furthermore, we can assign the structure at about 5 eV above threshold to F $1s \rightarrow 2e^*$. The shape resonance feature is broad because of the short lifetime of the resonance determined by the escaping time of the photoelectron temporally trapped by the molecular potential.

In Fig. 4, we report the yield curves for the singly charged species. Again we can observe that the spectral region related to Rydberg excitations acquires more relative intensity for the lighter fragments, although as is the case for the Si $L_{2,3}$ edge, there is no definite trend as a function of fragment mass.

We also notice that the intensity ratio between spectral features at 689.2 and 691.8 eV, related to transitions to the $6a_1$ and $6t_2$ molecular orbitals with σ^* (Si–F) character, changes very noticeably if we compare the different yield curves, while it varies much less for the corresponding curves obtained around the Si $L_{2,3}$ edges, where such intensity ratio (between the two groups of spin-orbit-split features at 106.095 and 106.650 eV and at 108.360 and 108.800 eV) is rather similar. Since the relative intensity of the peak at 691.8 eV seems to mimic the behavior of the following group of peaks, assigned as pure Rydberg transitions, at least in the majority of the yield curves, we can assess that this behavior is explained by the partial Rydberg character of such feature, while the corresponding features below the Si $L_{2,3}$ edges have a more pronounced molecular orbital character with little or no Rydberg contribution.

We can also notice that the above threshold structure which can be related to shape resonances are rather weak, especially compared to the Si $L_{2,3}$ edge. We can speculate that the trapping mechanism is more effective when the outgoing electron leaves from the central atom.

In Fig. 5, we show the yield curves for the doubly and triply charged fragments. The general trend is that the above threshold features are more intense, again in agreement with the assumption that the normal Auger decay following the shape resonance excitation produces doubly charged species. However, this is not a general trend; such structures are very intense only in a few of the yields of doubly charged species (F^{++}, Si^{++}, SiF^{++}), implying some extended fragmentation taking place at the shape resonance positions.

In Fig. 6, we report the yield curves for the negatively

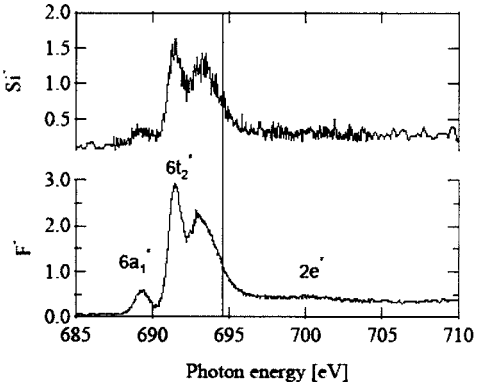

FIG. 6. Partial ion yields for all the negatively charged fragments detected around the F 1*s* edge.

charged species. It is interesting to notice that the shape resonance features are barely visible there, consistent with what we observed in Fig. 4. This is at variance with what we observed in SF_6, where the intensity of the shape-resonance-related features is comparable at the two edges. We can conclude that in the present case, the localization of the continuum feature around the central atom is higher, and therefore the resonant intensity is lower.

CONCLUSION

We reported experiments on partial ion yields upon core excitation around both the Si 2*p* and the F 1*s* core levels. We demonstrated that in such a relatively large system, the production of anions is possible in the shape resonance region, in analogy with our previous results on another rather large molecule with electronegative ligands, SF_6, and at variance with many smaller molecules (CO, CO_2, NO, N_2O). This can be related to the possibility in a relatively large system to dissipate positive charge over several channels. The shape resonances are clearly visible in the ion yields when the species is core excited around the Si 2*p* core level, while those are almost invisible when the excitation takes place around the F 1*s* core level. We attribute this finding to a more localized character of the continuum resonances around the central atom. We confirm our previous observation reported for other systems that the spectral region pertaining to the excitation to Rydberg states is more intense as a function of the extent of fragmentation.

ACKNOWLEDGMENTS

The authors thank the staff of the ALS for their excellent support. The research was funded by the National Science Foundation under Award No. PHY-01-40375, and the experiments were performed at the Advanced Light Source, which is supported by the Director, Office of Energy Research, Office of Basic Energy Sciences, Materials Sciences Division of the U.S. Department of Energy under Contract No. DE-AC03-76SF00098.

[1] M. N. Piancastelli, J. Electron Spectrosc. Relat. Phenom. **100**, 167 (1999), and references therein.
[2] J. L. Dehmer, J. Chem. Phys. **56**, 4496 (1972).
[3] R. E. Farren, J. A. Sheeny, and P. W. Langhoff, Chem. Phys. Lett. **177**, 307 (1991), and references therein.
[4] A. S. Vinogradov and T. M. Zimkina, Opt. Spektrosk. **31**, 288 (1971).
[5] J. L. Dehmer, J. Chem. Phys. **56**, 4496 (1972).
[6] M. Sugewara, *Plasma Etching: Fundamentals and Applications* (Oxford University Press, Oxford, 1988).
[7] M. Suto, X. Wang, L. C. Lee, and T. J. Chuang, J. Chem. Phys. **86**, 1152 (1987).
[8] K. Kameta, M. Ukai, T. Numazawa, N. Terazawa, Y. Chikahiro, N. Kouchi, Y. Hatano, and K. Tanaka, J. Chem. Phys. **99**, 2487 (1993).
[9] L. Cooper, L. G. Shpinkova, D. M. P. Holland, and D. A. Shaw, Chem. Phys. **270**, 363 (2001).
[10] D. M. P. Holland, A. W. Potts, L. Karlsson, A. B. Trofimov, and J. Schirmer, J. Phys. B **35**, 1741 (2002).
[11] B. W. Yates, K. H. Tan, G. M. Bancroft, L. L. Coatsworth, and J. S. Tse, J. Chem. Phys. **83**, 4906 (1985).
[12] X. Guo, G. Cooper, W.-F. Chan, G. R. Burton, and C. E. Brion, Chem. Phys. **161**, 453 (1992).
[13] G. G. B. de Souza, M. L. M. Rocco, H. M. Boechat-Roberty, C. A. Lucas, I. Borges, Jr., and E. Hollauer, J. Phys. B **34**, 1005 (2001).
[14] K. Kuroki, D. Spence, and M. A. Dillon, J. Electron Spectrosc. Relat. Phenom. **70**, 151 (1994).
[15] M. B. Robin, Chem. Phys. Lett. **31**, 140 (1975).
[16] T. A. Ferrett, M. N. Piancastelli, D. W. Lindle, P. A. Heimann, and D. A. Shirley, Phys. Rev. A **38**, 701 (1988).
[17] G. G. B. de Souza, P. Morin, and I. Nenner, J. Chem. Phys. **90**, 7071 (1989).
[18] G. M. Bancroft, S. Aksela, H. Aksela, K. H. Tan, B. W. Yates, L. L. Coatsworth, and J. S. Tse, J. Chem. Phys. **84**, 5 (1986).
[19] C. Miron, R. Guillemin, N. Leclercq, P. Morin, and M. Simon, J. Electron Spectrosc. Relat. Phenom. **93**, 95 (1998).
[20] G. C. King, M. Tronc, F. H. Read, and R. C. Bradford, J. Phys. B **10**, 2479 (1977).
[21] R. Puttner, M. Domke, K. Schultz, and G. Kaindl, Chem. Phys. Lett. **250**, 145 (1996) and references therein.
[22] F. Tarantelli and L. S. Cederbaum, Phys. Rev. Lett. **71**, 649 (1993).
[23] S. Bodeur, I. Nenner, and P. Millié, Phys. Rev. A **34**, 2986 (1986).
[24] S. Bodeur, P. Millié, and I. Nenner, Phys. Rev. A **41**, 252 (1990).
[25] K. Fujiwara, G. Prümper, A. De Fanis, Y. Tamenori, T. Tanaka, M. Kitajima, H. Tanaka, M. Oura, and K. Ueda, Chem. Phys. Lett. **402**, 17 (2005).
[26] D. A. Lapiano-Smith, C. I. Ma, K. T. Wu, and D. M. Hanson, J. Chem. Phys. **90**, 2162 (1989).
[27] M. Kitajima, A. De Fanis, K. Okada, H. Yoshida, H. Hoshino, H. Tanaka, and K. Ueda, J. Electron Spectrosc. Relat. Phenom. **144–147**, 199 (2005).
[28] K. Okada, Y. Tamenori, I. Koyano, and K. Ueda, Phys. Rev. Lett. **9**, 89 (2002), and references therein.
[29] J. D. Bozek, G. M. Bancroft, and K. H. Tan, Chem. Phys. **145**, 131 (1990).
[30] H. Ishikawa, K. Fujima, H. Adachi, E. Miyauchi, and T. Fujii, J. Chem. Phys. **94**, 6740 (1991).
[31] J. A. Tossell and J. W. Davenport, J. Chem. Phys. **80**, 813 (1984).
[32] D. Toffoli, M. Stener, and P. Decleva, Phys. Rev. A **73**, 042704 (2006), and references therein.
[33] M. N. Piancastelli, W. C. Stolte, R. Guillemin, A. Wolska, S.-W. Yu, M. M. Sant'Anna, and D. W. Lindle, J. Chem. Phys. **122**, 1 (2005).
[34] W. C. Stolte, D. L. Hansen, M. N. Piancastelli, I. Dominguez-Lopez, A. Rizvi, O. Hemmers, H. Wang, A. S. Schlachter, M. S. Lubell, and D. W. Lindle, Phys. Rev. Lett. **86**, 4504 (2001).
[35] S.-W. Yu, W. C. Stolte, G. Öhrwall, R. Guillemin, M. N. Piancastelli, and D. W. Lindle, J. Phys. B **36**, 1255 (2003).
[36] G. Öhrwall, M. M. Sant'Anna, W. C. Stolte, I. Dominguez-Lopez, L. T. N. Dang, A. S. Schlachter, and D. W. Lindle, J. Phys. B **35**, 4543 (2002).
[37] S.-W. Yu, W. C. Stolte, R. Guillemin, G. Öhrwall, I. C. Tran, M. N. Piancastelli, R. Feng, and D. W. Lindle, J. Phys. B **37**, 3583 (2004).
[38] W. C. Stolte, Y. Lu, J. A. R. Samson, O. Hemmers, D. L. Hansen, S. B. Whitfield, H. Wang, P. Glans, and D. W. Lindle, J. Phys. B **30**, 4489 (1997).
[39] M. N. Piancastelli, W. C. Stolte, G. Öhrwall, S.-W. Yu, D. Bull, K. Lantz, A. S. Schlachter, and D. W. Lindle, J. Chem. Phys. **117**, 8264 (2002).
[40] W. C. Stolte, M. M. Sant'Anna, G. Öhrwall, I. Dominguez-Lopez, M. N. Piancastelli, and D. W. Lindle, Phys. Rev. A **68**, 022701 (2003).
[41] D. Céolin, M. N. Piancastelli, R. Guillemin, W. C. Stolte, S.-W. Yu, O. Hemmers, and D. W. Lindle, J. Chem. Phys. **126**, 084309 (2007).